

# Molecular Weight and Molecular Weight Distribution Effects on the Liquid Crystalline and Biphasic Behavior of a Thermotropic Polyester

Michele Laus and A. Sante Angeloni

*Dipartimento di Chimica Industriale e dei Materiali, Viale Risorgimento 4, 40136 Bologna, Italy*

Giancarlo Galli and Emo Chiellini\*

*Dipartimento di Chimica e Chimica Industriale, Via Risorgimento 35, 56126 Pisa, Italy*

Received March 2, 1992

**ABSTRACT:** Several samples of a liquid crystalline semiflexible polyester 1 with different molecular weights ( $M_n = 2800$ –37 400) and molecular weight distributions ( $M_w/M_n = 1.30$ –2.35) were prepared. Two polymer blends were also obtained from 1 components with specifically designed  $M_n$  and  $M_w/M_n$  values. The liquid crystalline properties of the samples and their biphasic behavior at the nematic to isotropic phase transition were investigated. The melting and isotropization temperatures as well as the isotropization entropy increase with increasing number average molecular weight until a saturation value for about  $M_n = 10\,000$  is reached. Beyond this value, they remain constant. The biphasic behavior was studied by annealing the samples inside the apparent nematic to isotropic biphasic gap. The onset and extension of the biphasic segregation is critically affected by the molecular weight and molecular weight distribution with a clear cut at intermediate values of these parameters. In particular, the position of the biphasic region depends on the number average molecular weight, whereas the width of the biphasic region depends on the width of the molar mass distribution.

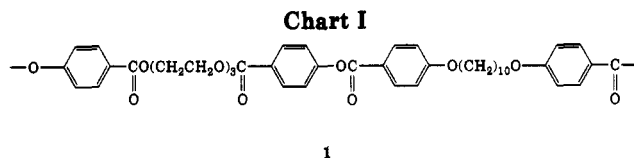
## Introduction

A substantial body of experimental and theoretical work has been devoted to the investigation of the thermodynamic and kinetic aspects of the isotropic–anisotropic biphasic equilibria in thermotropic liquid crystalline polymeric systems. The occurrence of a thermodynamically stable biphasic region situated between the pure nematic phase and the pure isotropic phase has been described in semiflexible main-chain polymers with regular<sup>1–5</sup> or statistical<sup>6–9</sup> distribution of rigid and flexible segments along the polymer backbone. Very recently, the observation of the nematic–isotropic and smectic–nematic biphasic behavior has also been reported for side-chain liquid crystalline polymers.<sup>10</sup> The coexistence of nematic and isotropic phases over a finite range of temperatures is unambiguously indicative of the multicomponent nature of the polymeric systems. However, the structural and molecular factors conducive to incompatibility in the melt and the driving force for macrophase segregation are still to be properly assessed.

Several different segregation mechanisms should be considered to account for the nematic to isotropic biphasic separation process. The chemical heterogeneity of main-chain polymers with statistical distribution of comonomer units is suggested to produce a distribution of persistence lengths, strictly connected to a distribution of chain flexibilities, so called polyflexibility, capable of promoting partitioning between the two liquid phases with the more rigid chain molecules being selectively incorporated into the anisotropic phase. Theoretical calculations<sup>11,12</sup> are in agreement with the above explanation of the biphasic behavior of liquid crystalline statistical copolymers.

In contrast, the nematic to isotropic biphasic behavior of main-chain polymers with regular structure is primarily ascribed to the molecular weight polydispersity of the samples. A preferential retention of the longer chain molecules into the anisotropic phase is observed.

In previous work<sup>4,5</sup> we have shown that in a thermotropic polyester such as polymer 1 (Chart I) containing a



regular sequencing of rigid anisometric units and flexible spacer segments, there occurs a biphasic region at the isotropization transition, where the nematic melt and the isotropic liquid coexist at equilibrium. The two components segregated macroscopically and were individually analyzed, thus showing that the nematic phase had enriched in higher molecular weight species, whereas lower molecular weight chains had been preferentially retained in the isotropic phase. Furthermore, optical microscopy observations permitted the detection of the phase segregation process and the distinct phase transitions of the separated phases during sequential heating/cooling cycles.<sup>4</sup> These results have stimulated further investigations into the dependence of the liquid crystalline properties and the biphasic behavior on the molecular weight ( $M_n$ ) and molecular weight dispersity ( $M_w/M_n$ ) of polymer 1 samples. Both these parameters may in general be expected to play a role in defining the position and extent of the biphasic at the isotropization transition in mesomorphic polymers.

We have synthesized and studied several samples of polymer 1 with different molecular weights and molecular weight distributions (1a–1l). Two polymer “blends” (1m and 1n) were also obtained by mixing specifically designed polymer 1 components and, therefore, exhibited predetermined molecular weight parameters ( $M_n$  and  $M_w/M_n$ ) for the study of their biphasic behavior.

## Experimental Part

**Synthesis.** Polymer samples 1c, 1e, and 1h with different molecular weights were prepared, according to the procedure previously reported,<sup>13</sup> by a condensation reaction under phase-transfer conditions. The synthetic route is outlined in Scheme I. In a typical polymerization reaction, a solution of 2.50 g (0.0055 mol) of 4,4'-(decamethylenedioxy)bis[benzoic acid chloride] (2)

in 50 mL of anhydrous 1,2-dichloroethane was added to a solution containing 2.16 g (0.0055 mol) of 3,6-dioxaoctane-1,8-diylbis[4-hydroxybenzoate] (3), 1.00 g (0.003 mol) of benzyl tributylammonium bromide, and the appropriate amount of sodium hydroxide in 50 mL of water. The sodium hydroxide/diphenol mole ratios employed were 2.0 for sample 1c, 4.0 for sample 1e, and 8.0 for sample 1h. The mixture was vigorously stirred for 15 min and then poured into 300 mL of methanol. The precipitated polymer 1 was washed with methanol and diethyl ether and purified by precipitations from chloroform solution into methanol. Polymer yields were higher than 85% in any polymerization experiment.

Polymer samples 1c and 1h were fractionated by preparative high-pressure size exclusion chromatography, the former giving samples 1a, 1b, and 1d and the latter giving samples 1f, 1g, 1i, and 1l. A liquid chromatograph, consisting of a Waters 590 pump, a Waters U6K injector, a Waters R-401 differential refractometer, and a fraction collector, equipped with a preparative Shodex H-2004 column was used. The eluent was chloroform with a flow rate of 4 mL min<sup>-1</sup>. Each sample was fractionated 10 separate times (50 mg each). The fractions with identical elution times were combined, and the solvent was evaporated under vacuum.

Polymer blends 1m and 1n were prepared by dissolving equimolar amounts (100 mg of each individual component) of samples 1c and 1h and samples 1d and 1i, respectively, in 10 mL of chloroform. The chloroform mixtures were gently stirred until completely dissolved. The chloroform was then evaporated, and the blends were dried at least 1 week in a vacuum oven at room temperature. To make sure of the complete homogenization, the polymer blends were heated to 433 K in the isotropic phase and maintained 3 h at this temperature before making measurements.

**Characterization.** The molecular weights of the polymers were measured by the above liquid chromatograph apparatus using an analytical Shodex KF-804 column. Chloroform was used as the eluent with a flow rate of 1 mL min<sup>-1</sup>. Polystyrene standard samples were employed for the universal calibration method.<sup>14</sup> Molecular weight values were corrected for the axial dispersion. Differential scanning calorimetry (DSC) analyses were carried out under dry nitrogen flow with a Perkin-Elmer DSC 7 apparatus. Samples of 5–10 mg were employed. The temperature scale was calibrated against the melting temperatures of *n*-hexane, benzoic acid, and indium. For the determination of the transition enthalpy, indium was used as a standard material. The transition temperatures were taken from the DSC traces of samples annealed by cooling from the isotropic melt, as corresponding to the maximum/minimum of the enthalpic peaks at a heating/cooling rate of 10 K min<sup>-1</sup>. The nematic to isotropic transition parameters of samples in which the melting and isotropization endotherms were partly overlapped, were calculated by cooling the samples to just below the isotropic to nematic transition and then heating at 10 K min<sup>-1</sup> to the isotropic phase.

The biphasic behavior was studied by DSC according to the procedure previously described.<sup>4</sup> A sample of polymer 1 was heated for 20 min at 433 K in the isotropic phase. Subsequently, the sample was cooled at 1 K min<sup>-1</sup> to a selected temperature in the biphasic region, maintained at this temperature for 15 h and then rapidly cooled to room temperature or to a temperature far away from incipient crystallization and finally subjected to several heating/cooling cycles at 10 K min<sup>-1</sup>. The annealing time of 15 h was found<sup>4</sup> to be optimal to achieve the best separation without any appreciable chain degradation process. For each annealing temperature a fresh polymer sample was employed. DSC traces were normalized to a 1-mg sample. Optical microscopy observations were performed on polymer films between glass slides by means of a Reichert Polyvar microscope equipped with a programmable Mettler FP52 heating stage at a scanning rate of 10 K min<sup>-1</sup>.

## Results and Discussion

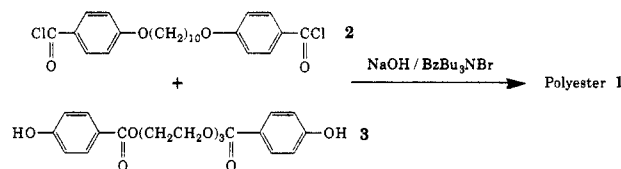
**Synthesis.** Polymer samples 1c, 1e, and 1h with different molecular weights were prepared by a condensation reaction between the 4,4'-(decamethylenedioxy)-

**Table I**  
Physicochemical and Liquid Crystalline Properties of Polymer 1 Samples

| sample | $M_n^a$ | $M_w/M_n^a$ | $T_m$ ,<br>K | $T_i^b$ ,<br>K | $\Delta H_i$ ,<br>kJ mol <sup>-1</sup> | $\Delta S_i$ ,<br>J mol <sup>-1</sup> K <sup>-1</sup> |
|--------|---------|-------------|--------------|----------------|--|---|
| 1a     | 2800    | 1.49        | 407          | 411            | 4.8                                    | 11.7  |
| 1b     | 3700    | 1.36        | 410          | 414            | 5.4                                    | 13.0  |
| 1c     | 3900    | 1.63        | 409          | 412            | 5.9                                    | 14.3  |
| 1d     | 5900    | 1.27        | 413          | 418            | 6.9                                    | 16.5  |
| 1e     | 10100   | 2.34        | 414          | 422            | 7.6                                    | 18.0  |
| 1f     | 11800   | 1.84        | 415          | 427            | 7.4                                    | 17.3  |
| 1g     | 15000   | 1.76        | 416          | 427            | 7.5                                    | 17.6  |
| 1h     | 15400   | 1.97        | 413          | 427            | 7.4                                    | 17.3  |
| 1i     | 21200   | 1.47        | 415          | 427            | 7.6                                    | 17.8  |
| 1l     | 37400   | 1.30        | 415          | 429            | 7.8                                    | 18.2  |
| 1m     | 8700    | 2.35        | 413          | 420            | 7.3                                    | 17.4  |
| 1n     | 8400    | 1.95        | 414          | 421            | 7.5                                    | 17.8  |

<sup>a</sup> By SEC, in chloroform at 30 °C. <sup>b</sup> Isotropization (nematic to isotropic) transition temperature, by DSC (10 K min<sup>-1</sup>).

**Scheme I**



bis[benzoic acid chloride] (2) in 1,2-dichloroethane solution and the sodium salt of 3,6-dioxaoctane-1,8-diylbis[4-hydroxybenzoate] (3) in water solution using benzyl tributylammonium bromide as the phase-transfer agent (Scheme I).

The molecular weight parameters of these samples were controlled by appropriate adjustment of the sodium hydroxide/diphenol mole ratios employed. Increasing this ratio from 2.0 to 8.0 resulted in a marked increase in the number average molecular weights from  $M_n = 3900$  to 15 400 (Table I).

Polymer sample 1c was separated into three fractions (1a, 1b, and 1d) and polymer sample 1h was separated into four fractions (1f, 1g, 1i, and 1l) by preparative high-pressure size exclusion chromatography (SEC). Figure 1 shows the SEC curves of the molecular weight distributions of the polymer fractions so obtained as well as those of the original unfractionated polymers. The relevant molecular weight parameters are collected in Table I. The shapes of the distribution curves of the various fractions are comparable to each other. The number average molecular weight values of the polymer fractions range from  $M_n = 2800$  to 37 400, with the first polydispersity index between  $M_w/M_n = 1.27$  and 1.84.

Two polymer blends 1m and 1n were also prepared by mixing equimolar amounts of samples 1c and 1h with relatively broad molar mass distributions and fractions 1d and 1i with narrow molar mass distributions, respectively. These polymer-blended samples have the same number average molecular weight ( $M_n = 8700$  and 8400) but differ substantially in their molar mass distributions ( $M_w/M_n = 2.35$  and 1.95, Table I).

**Liquid Crystalline Properties.** The thermal and liquid crystalline behaviors of the various polymer samples were studied by combined differential scanning calorimetry and optical microscopy observations. The phase transition parameters were determined on samples that had been annealed by cooling at 10 K min<sup>-1</sup> from the isotropic melt (Table I). Representative DSC heating curves of samples with different molecular weights and molecular weight distributions are reported in Figure 2. Generally, a weak cold-crystallization exotherm at about

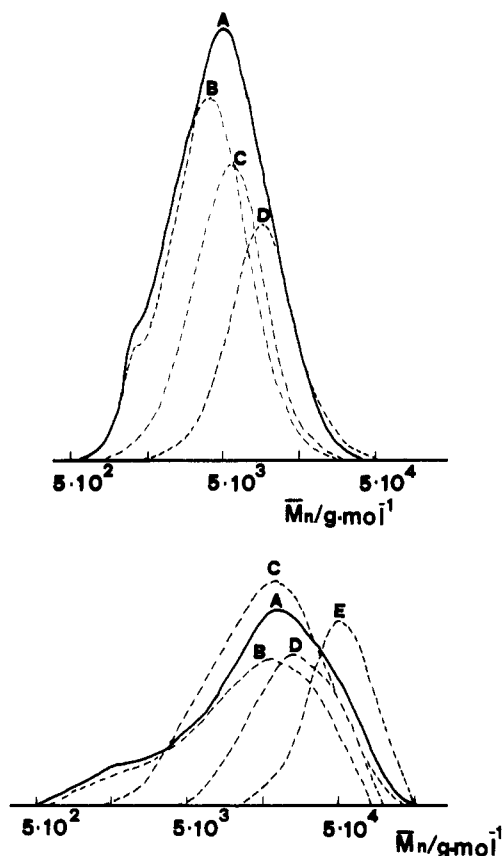


Figure 1. SEC traces of polymer 1 samples: (a, top) A, 1c; B, 1a; C, 1b; D, 1d; (b, bottom) A, 1h; B, 1f; C, 1g; D, 1i; E, 1l.

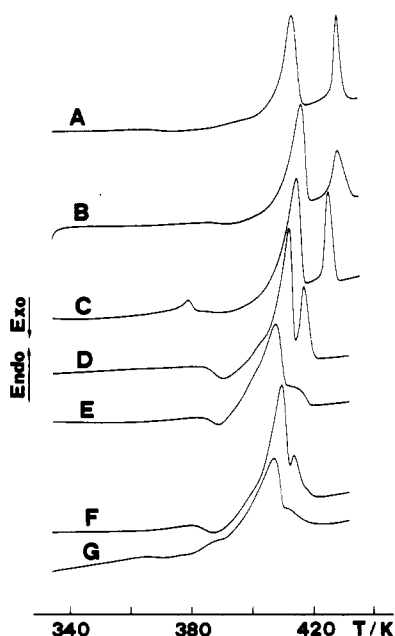


Figure 2. DSC heating curves ( $10\text{ K min}^{-1}$ ) for polymer 1 samples with different molecular weights and molecular weight distributions: A, 1l; B, 1h; C, 1g; D, 1d; E, 1c; F, 1b; G, 1a.

405 K precedes two endothermic transitions attributed to the crystal melting and to the nematic to isotropic transition. The nematic to isotropic transition endotherm is partly overlapped to the crystal melting endotherm for the lower molecular weight samples, whereas it emerges progressively better resolved with increasing molecular weight. Upon cooling, two exothermic transitions assigned to the isotropic to nematic transition and to the crystallization occur. The DSC heating traces of polymer blends 1m and 1n are very similar to those of the samples so far described and practically superimposable to each other.

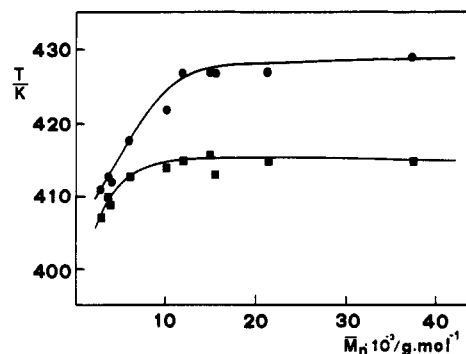


Figure 3. Trends of the melting (■) and isotropization temperatures (●) for polymer 1 samples as function of the number average molecular weight  $M_n$ .

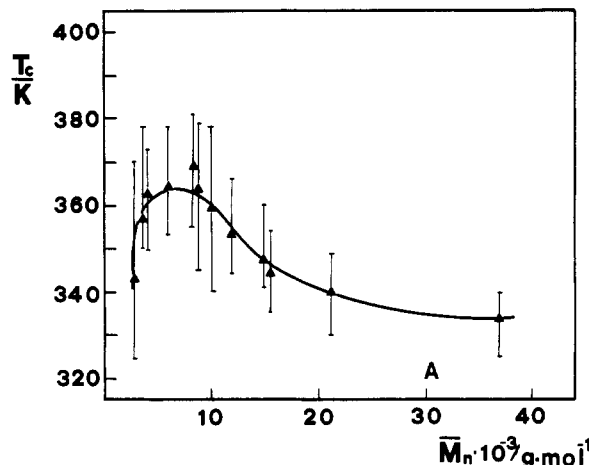
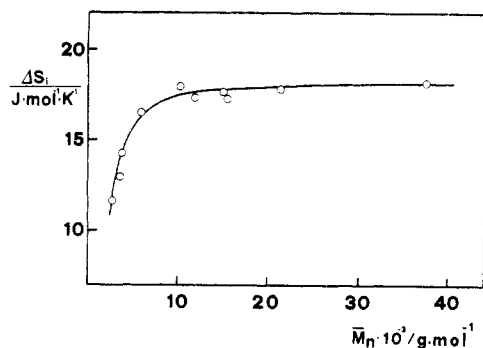


Figure 4. Trend of the crystallization temperature  $T_c$  and crystallization range for polymer 1 samples as a function of the number average molecular weight  $M_n$ , by DSC ( $10\text{ K min}^{-1}$ ).

The only difference is observed in the DSC cooling curves. The crystallization exotherm of polymer blend 1m, which has the wider molar mass distribution, occurs with a greater degree of supercooling and is broader than the corresponding transition exotherm of polymer blend 1n.

The trends of the transition temperatures as function of the number average molecular weight are illustrated in Figure 3. The melting and the nematic to isotropic transition temperatures increase, steeply at first and then more gradually, with increasing molecular weight, up to a saturation value for about  $M_n = 10\,000$ . Beyond this value, the transition temperatures remain constant. The increase in the isotropization temperature with molecular weight is more pronounced than the one in the melting temperature and accordingly wider mesophasic ranges are observed for polymer samples with higher molecular weight values. The crystallization temperature, taken as corresponding to the minimum of the crystallization exotherm and the width of the relevant peak of the various samples as a function of the number average molecular weight are reported in Figure 4. There is typically a supercooling degree greater than 50 K. Initially, the crystallization temperature increases with molecular weight from 343 to 368 K, thus reflecting a decreasing influence of the chain ends, and then, after reaching the maximum value corresponding to an intermediate molecular weight of 7000–8000 it decreases to 338 K. This is probably due to the increased viscosity of the melt. In contrast, the isotropic to nematic phase transition occurs with a supercooling of a few degrees (5–8 K), irrespective of the molecular weight of the samples. These results indicate that the liquid crystalline phase transition is mainly thermodynamically controlled, whereas the crystalline phase transition is kinetically controlled.



**Figure 5.** Trend of the isotropization entropy for polymer 1 samples as a function of the number average molecular weight  $M_n$ .

The trend of the isotropization entropy as a function of the number average molecular weight (Figure 5) closely parallels the one of the isotropization temperature. The isotropization entropy increases with molecular weight from  $11.7 \text{ J mol}^{-1} \text{ K}^{-1}$  up to a saturation value of  $17.5 \text{ J mol}^{-1} \text{ K}^{-1}$ , corresponding to the same molecular weight of about 10 000, and beyond this value it remains constant.

The increase in the nematic to isotropic phase transition parameters with molecular weight has been reported in a variety of main-chain thermotropic polymers<sup>15–19</sup> and is ascribed to an increased cooperativity between distant units belonging to the same macromolecular chain, brought about by the orientational field associated with the mesomorphic order.<sup>20,21</sup> This cooperative alignment of neighboring rigid groups in the nematic state increases the overall rigidity of the polymer backbone and consequently imparts an increasing first-order character to the nematic to isotropic phase transition. It should be noted that the polydispersity of the various samples appears to be of limited importance in determining the molecular weight dependence of the nematic to isotropic transition parameters.

**Biphasic Behavior.** The biphasic behavior at the nematic to isotropic phase transition of polymer 1 samples with different molecular weights and molecular weight distributions, including the two polymer blends, was studied by differential scanning calorimetry, in analogy to ref 4, according to the following thermal procedure. All the samples were heated to the isotropic phase at 433 K, slowly cooled to the predetermined annealing temperature ( $T_a$ ) in the range 412–424 K inside the apparent nematic to isotropic biphasic gap, maintained at this temperature for 15 h, and then rapidly cooled to room temperature. It was previously demonstrated<sup>4</sup> that under these experimental conditions no appreciable transesterification or sequence randomization processes took place. In Figures 6 and 7 are reported the DSC heating curves of polymer blends 1m and 1n, respectively, following annealing at various temperatures. Below each continuous curve, there is a dashed curve which is obtained, after annealing in the biphasic region as above, by cooling the sample to a temperature far away from incipient crystallization and then heating up to complete isotropization. In both polymer blends, within the annealing temperature range reported, the isotropization peak appears structured into two components. For the lower annealing temperatures, the lower isotropization temperature component appears completely overlapped by the melting endotherm and accordingly the transition is partly monotropic and partly enantiotropic in nature. The DSC cooling curves are practically the mirror images of the corresponding DSC heating curves and two isotropic to nematic and one crystallization exotherm are observed.

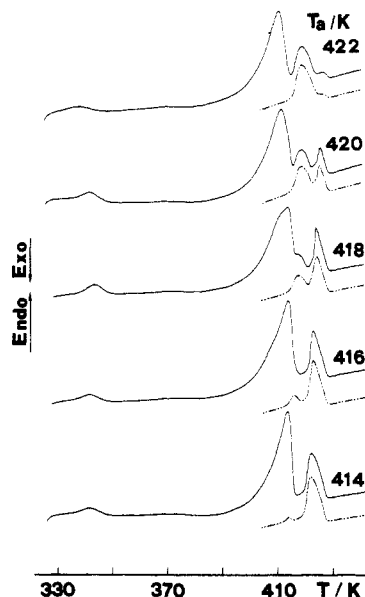


**Figure 6.** DSC heating curves ( $10 \text{ K min}^{-1}$ ) for the 1m blend following annealing at different temperatures  $T_a$  in the biphasic (annealing time = 15 h).

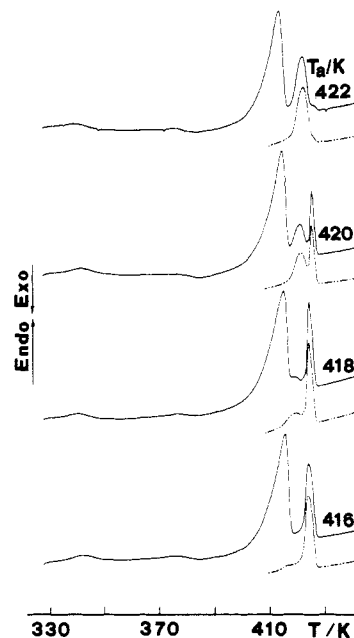


**Figure 7.** DSC heating curves ( $10 \text{ K min}^{-1}$ ) for 1n blend following annealing at different temperatures  $T_a$  in the biphasic (annealing time = 15 h).

This dual isotropization behavior reflects the occurrence of a biphasic separation process in which the lower and higher molecular weight fractions of the polymer segregate during annealing in the biphasic region, the latter segregating into the component with the higher transition temperature.<sup>4</sup> The above thermal procedure permits estimation of the thermodynamic biphasic gap associated to the nematic to isotropic phase transition and delineation of the distribution of the volumes of the two coexisting phases at equilibrium. The peak temperatures of the isotropization endotherms and the volume fractions of the isotropic component following demixing in the biphasic region as a function of  $T_a$  are reported in Figures 8 and 9, respectively. For each sample, the peak temperatures of both isotropization endotherms regularly increase with annealing temperature (Figure 8). This indicates that the average molecular weight of both segregated polymer fractions increases with increasing annealing temperature. By comparison of the trends of the isotropization peak

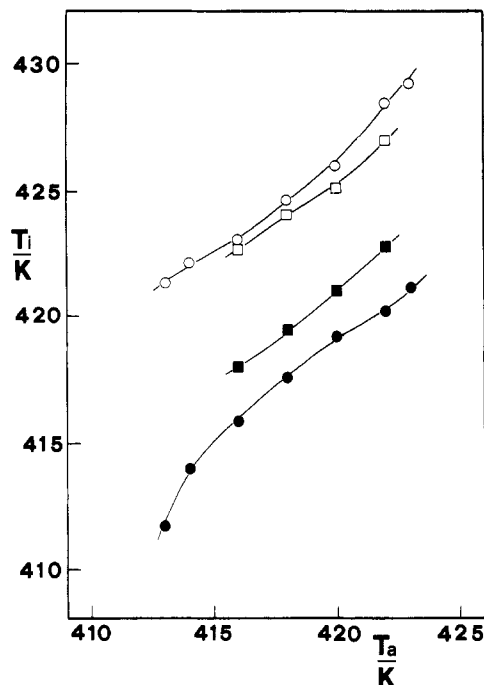


**Figure 8.** Nematic to isotropic transition temperatures for the formerly nematic component in the biphasic (open symbols) and formerly isotropic component in the biphasic (full symbols) for 1m (○, ●) and 1n (□, ■) blends following demixing (annealing time = 15 h) as a function of the annealing temperature  $T_a$ .

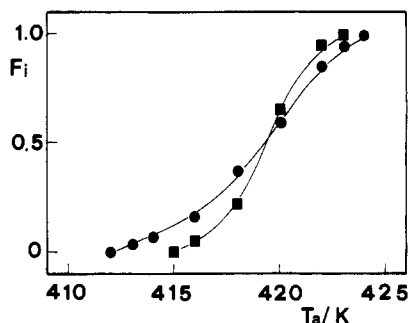


**Figure 9.** Volume fractions of the isotropic component ( $F_i$ ) for 1m (●) and 1n (■) blends following demixing (annealing time = 15 h) as a function of the annealing temperature  $T_a$ .

temperature and the volume fraction of the isotropic component of polymer blends as a function of  $T_a$ , it appears that the biphasic regions of both polymer blends are centered near the same temperature ( $F_i = 0.5$  at 420 K in Figure 9), but the width of the biphasic region and the average separation between the isotropization peak temperatures are larger for polymer blend 1m consisting of a wider molecular weight distribution.

The biphasic behavior of polymer samples 1e and 1h was previously investigated<sup>4,5</sup> by the same annealing procedure and is compared to the one of polymer sample 1f which shows a thermal behavior very similar to those of polymer blends 1m and 1n. The trends of the isotropization peak temperatures and the volume fraction of the isotropic component following demixing in the nematic to isotropic biphasic region of samples 1e, 1f, and 1h as a function of  $T_a$  are reported in Figures 10 and 11, respectively. The position of the biphasic region moves to higher temperature values with an increasing number average molecular weight of the polymer samples, while the width and average separation of the isotropization peak temperatures appear to be directly correlated to the width of the molecular weight distribution.

All the other (1a, 1b, 1c, 1d, 1g, 1i, and 1l) samples were subjected to the same annealing treatment, but rather

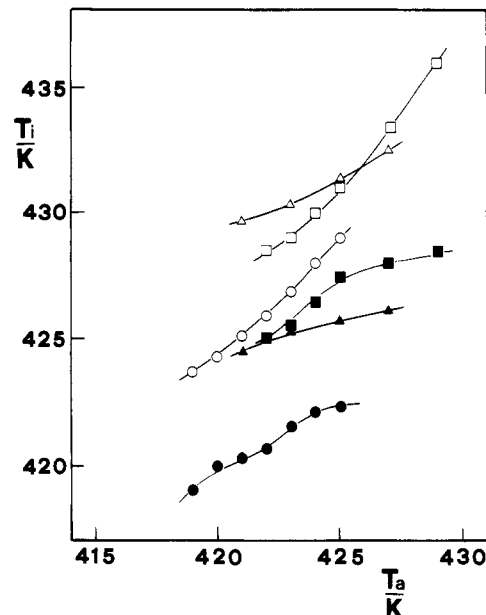


**Figure 10.** Nematic to isotropic transition temperatures for the formerly nematic component in the biphasic (open symbols) and formerly isotropic component in the biphasic (full symbols) for 1e (○, ●), 1f (△, ▲), and 1h (□, ■) polymer samples following demixing (annealing time = 15 h) as a function of the annealing temperature  $T_a$ .

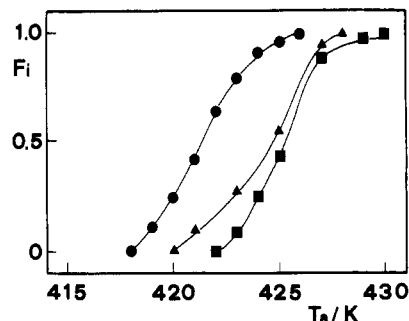


**Figure 11.** Volume fractions of the isotropic component ( $F_i$ ) for 1e (●), 1f (▲), and 1h (■) polymer samples following demixing (annealing time = 15 h) as a function of the annealing temperature  $T_a$ .

surprisingly, in none of these cases was the nematic to isotropic biphasic separation observed even after annealing for long periods of time in their entire apparent biphasic regions.

### Concluding Remarks

Several samples of polymer 1 with different molecular weight and molecular weight distribution were prepared and studied with respect to their liquid crystalline properties and biphasic behavior at the nematic to isotropic phase transition. While the liquid crystalline transition was found to be mainly thermodynamically controlled, the crystalline transition displayed a rather pronounced off-equilibrium character, as usually occurring in thermotropic polymers. Both the melting and nematic to isotropic phase transition temperatures increase with increasing number average molecular weight up to a saturation value corresponding to about  $M_n = 10\,000$ . Beyond this value, they remain constant irrespective of the width of the molecular weight distribution of the samples. The same trend is also shown by the isotropization entropy. Note that the  $M_n$  limiting value of 10 000 appears to be a general threshold in main-chain liquid crystalline polymers independent of the repeat unit structure.

The biphasic behavior at the nematic to isotropic transition was studied by annealing the samples inside the apparent biphasic gap. While this behavior had been previously investigated in a few polymeric systems,<sup>1-5</sup> in this work the study was extended for the first time to polymer "blends" with specifically designed molecular weights and degrees of polydispersity. Samples with high molecular weights ( $M_n > 20\,000$ ) and narrow molecular weight distributions ( $M_w/M_n < 1.5$ ) and samples with low molecular weights ( $M_n < 6000$ ) and narrow or relatively wide molecular weight distributions ( $M_w/M_n < 1.7$ ) do not show nematic to isotropic biphasic separation. In contrast, samples with intermediate molecular weights ( $M_n = 8000$ – $15\,000$ ) and relatively narrow or wide molar mass distributions ( $M_w/M_n = 1.7$ – $2.4$ ) show nematic to isotropic biphasic separation. Therefore, this phase separation appears to be due to the effects of the molecular weight and the molecular weight distribution of the polymer. The position of the biphasic region depends on the number average molecular weight, whereas the width of the biphasic region and the separation between the isotropization peak temperatures of the biphasic demixed components depend on the width of the molar mass distribution.

From these results we may infer that two conditions should be fulfilled for realizing the nematic to isotropic biphasic separation in semiflexible main-chain polymers with regular structure. The phase-transition parameters of the individual species constituting the polymer sample should differ substantially, according to their distinct molecular weight dependences. In addition, the average molecular weight of the sample should be fairly high. The latter condition suggests that the nematic to isotropic biphasic segregation process is mainly driven by a screening mechanism of entropic origin, in which the longer chain molecules segregate from the lower molar mass species, rather than by the difference in the inherent flexibility of the chain molecules with different molecular weights. In fact, the greatest difference in the flexibility of the individual species should be in the low molecular weight region where, however, no nematic to isotropic biphasic separation is detectable.

To further substantiate this conclusion, we are presently extending our investigation to polymorphic (nematic and smectic) thermotropic main-chain as well as side-chain polymers with controlled molecular weights and molecular weight distributions.

**Acknowledgment.** This work was supported by the "Progetto Finalizzato Chimica Fine II" of the National Research Council of Italy (CNR).

## References and Notes

- (1) D'Allest, J. F.; Wu, P. P.; Blumstein, A.; Blumstein, R. B. *Mol. Cryst. Liq. Cryst. Lett.* **1986**, *3*, 103.
- (2) D'Allest, J. F.; Sixou, P.; Blumstein, A.; Blumstein, R. B. *Mol. Cryst. Liq. Cryst.* **1988**, *157*, 229.
- (3) Kim, D. Y.; D'Allest, J. F.; Blumstein, A.; Blumstein, R. B. *Mol. Cryst. Liq. Cryst.* **1988**, *157*, 253.
- (4) Laus, M.; Caretti, D.; Angeloni, A. S.; Galli, G.; Chiellini, E. *Macromolecules* **1991**, *24*, 1459.
- (5) Chiellini, E.; Galli, G.; Laus, M.; Angeloni, A. S.; Caretti, D. *Mol. Cryst. Liq. Cryst.* **1992**, *215*, 101.
- (6) Moore, J. S.; Stupp, S. I. *Macromolecules* **1987**, *20*, 273, 282.
- (7) Moore, S. J.; Stupp, S. I. *Macromolecules* **1988**, *21*, 1217.
- (8) Martin, P. G.; Stupp, S. I. *Macromolecules* **1988**, *21*, 1222.
- (9) Stupp, S. I.; Moore, J. S.; Martin, P. G. *Macromolecules* **1988**, *21*, 1228.
- (10) Galli, G.; Chiellini, E.; Laus, M.; Caretti, D.; Angeloni, A. S. *Makromol. Chem., Rapid Commun.* **1991**, *12*, 43.
- (11) Fredrickson, G. H. *Macromolecules* **1989**, *22*, 2746.
- (12) Fredrickson, G. H.; Leibler, L. *Macromolecules* **1990**, *23*, 531.
- (13) Caretti, D.; Angeloni, A. S.; Laus, M.; Chiellini, E.; Galli, G. *Makromol. Chem.* **1989**, *190*, 1655.
- (14) Tung, L. H. *Fractionation of Synthetic Polymers*; Marcel Dekker: New York, 1977.
- (15) Krigbaum, W. R.; Ishikawa, T.; Watanabe, J.; Toriumi, H.; Kubota, K.; Preston, J. J. *Polym. Sci., Polym. Phys. Ed.* **1983**, *21*, 1851.
- (16) Blumstein, R. B.; Stickles, E. M.; Gauthier, M. M.; Blumstein, A.; Volino, F. *Macromolecules* **1984**, *17*, 177.
- (17) Galli, G.; Chiellini, E.; Angeloni, A. S.; Laus, M. *Macromolecules* **1989**, *22*, 1120.
- (18) Laus, M.; Angeloni, A. S.; Galli, G.; Chiellini, E. *Makromol. Chem.* **1990**, *191*, 147.
- (19) Percec, V.; Keller, A. *Macromolecules* **1990**, *23*, 4347.
- (20) Sigaud, G.; Yoon, Y. D.; Griffin, A. C. *Macromolecules* **1983**, *16*, 875.
- (21) de Gennes, P. G. *Mol. Cryst. Liq. Cryst. Lett.* **1984**, *102*, 95.

**Registry No.** 1 (copolymer), 123467-37-8; 1 (SRU), 119846-19-4.